 

# Microstructural and Mechanical Characterization of WAAM-fabricated Inconel 625: Heat Treatment Effects

Saravanakumar Krishnasamy ✉ – Saravanan Sambasivam – Balaji Vaiyampalayam Govindaraj

PSG College of Technology, Department of Production Engineering, India

✉ ksaravanakumr@gmail.com

**Abstract** *Wire arc additive manufacturing (WAAM) is a promising technique for producing complex geometries of nickel-based superalloys, such as Inconel 625. In this work, the microstructure and mechanical properties of Inconel 625 alloy produced by gas tungsten arc welding (GTAW) process of WAAM technology were analyzed to investigate the effects of heat treatment on the top and bottom zones of the multi-layered wall structure. The deposited specimens were heat treated at 980 °C for 2 hours, then water quenched (solution annealing). After heat treatment, microstructure reveals that the most common phases like laves, gamma, and mono carbides (MC) are dissolved, which is clear by optical microscopy (OM), scanning electron microscopy (SEM), and energy dispersive spectroscopy (EDS). Even after the heat treatment process, mechanical properties, such as micro-hardness results, demonstrate that the bottom zone of the multilayer wall structure has a higher hardness value than the top zone. After the secondary phases were eliminated by the solution annealing procedure, the ultimate tensile strength and yield strength were increased by nearly 17 % to 38 % and 15 % to 22 % in the top and bottom one of the multilayer wall structures, respectively.*

**Keywords** *wire arc additive manufacturing (WAAM), heat treatment, optical microscope, tensile strength*

**Highlights**:
- *WAAM with GTAW used to build multiwall Inconel 625 nickel-based superalloy structures.*
- *Heat treatment at 980 °C for 2 hours followed by water quenching was applied.*
- *Phases like Laves, gamma, and MC carbides dissolved after heat treatment.*
- *Hardness and strength improved; tensile strength increased by 17 % to 38 % after annealing.*

## 1 INTRODUCTION

Additive manufacturing (AM) has revolutionized the production of components with complex shapes, offering increased production flexibility and efficiency [1]. This method allows for the creation of fully dense parts using engineering and industrial materials such as steel, titanium, and aluminium [2]. wire arc additive manufacturing (WAAM) is a type of additive manufacturing (AM) that uses a digital model to build complex metal parts by melting and adding metal wire to the base material [3]. WAAM differs from powder-bed fusion systems, such as laser and electron beam ones, since it uses wire feedstock instead of powder [4]. WAAM has several advantages over powder-based AM technologies, including more availability of wire feedstock, cost-effectiveness, higher quality feedstock and deposition, and less work-in-progress waste [4]. Laser bed fusion and wire arc additive have their own advantages and disadvantages, and the choice between them depends on the specific requirements of the project. Laser powder bed fusion is better for small to medium-sized components with high detail and internal features, while WAAM is more suitable for large builds and customized objects with decent precision and accuracy [3] and [4]. Particularly, arc-welding-based additive manufacturing techniques, like WAAM, have gained popularity in the manufacturing industry for their ability to assemble large metal components quickly and cost-effectively [5]. WAAM utilizes an electrical arc as a heat source to melt and deposit filler wire layer by layer, creating near-net structure components. The process has successfully produced massive metallic components, demonstrating its potential for cost-effective manufacturing [6]. Three main types of WAAM processes exist: gas tungsten arc welding (GTAW), gas metal arc welding (GMAW), and plasma arc welding (PAW). GMAW boasts a higher deposition rate (2 to 3 times) compared to GTAW or PAW, but it comes with drawbacks such as instability, increased weld smoke, and spatter [7]. On the other hand, GTAW-based WAAM provides direct control over energy and material inputs, allowing for more stable welding. Unlike traditional automatic welding, GTAW WAAM follows a non-unidirectional welding path [8].

AM technologies, such as direct laser deposition (DLD), microplasma additive manufacturing (MPAM), and cold metal transfer wire arc additive manufacturing (CMT-WAAM), have garnered significant attention in the manufacturing industry due to their ability to produce complex metal parts with high precision and minimal material waste. Among these technologies, WAAM, particularly the cold metal transfer (CMT) variant, has shown notable advancements in the production of heat-resistant superalloys like Inconel 625, making it a preferred method for manufacturing components that require high strength and durability under extreme conditions [9] and [10].

Crucial parameters influencing the WAAM process with GTAW include welding current, voltage, polarity, gas flow rate, welding speed, and electrode tip angle [11]. Inconel 625, a nickel-based superalloy renowned for its exceptional corrosion resistance, high strength, and toughness, finds applications across various industries like aerospace, chemical processing, and marine engineering. When produced using WAAM, Inconel 625 exhibits a microstructure characterized by elongated crystallites, accompanied by favorable mechanical properties [12]. WAAM offers several advantages, including high energy density, excellent surface forming capabilities, and the ability to customize microstructures by adjusting process parameters. Refractory metals like niobium and molybdenum, present in nickel-chromium alloys, contribute to solid-solution hardening, further enhancing the properties of alloys like Inconel 625 [13].

The CMT discontinuous WAAM strategy, in particular, allows for lower heat input and improved control over the welding process, leading to finer details and enhanced performance in thin-walled components. Recent studies have demonstrated that this method can significantly improve the material properties of Inconel 625, including a 15 % increase in ultimate tensile strength at room temperature and improved wear resistance at elevated temperatures [14] and [15].

The selection of Inconel 625 for this study is based on its exceptional properties, including high strength, corrosion resistance, and weldability, which are essential for applications requiring durability under extreme conditions. The alloy's higher nickel content compared to other Inconel grades enhances its performance in high-temperature environments, making it a preferred choice in sectors like aerospace and chemical processing. Furthermore, the ability to fabricate complex shapes directly from digital models using WAAM provides significant advantages in design flexibility and material utilization, which are critical in modern engineering applications. As the research into Inconel 625 continues to evolve, the findings not only contribute to the understanding of additive manufacturing techniques but also support the development of innovative solutions for high-performance engineering challenges [9], [10], [14], and [15].

Studies exploring Inconel 625 production using WAAM techniques have shown diverse results. A low heat input WAAM process with a metal inert gas technique demonstrated increased hardness, while a pulsed tungsten inert gas (TIG) welding process with activated flux improved penetration and tensile strength [16]. Additionally, WAAM-produced Inconel 625 alloys exhibited favorable microstructure, forming quality, and metallurgical bonding, with Ni and granular precipitated phases identified and promising microhardness values reported [17]. The WAAM method has been extended to create functionally gradient materials, such as SS321/Inconel 625, with minimal interface issues. The resulting alloy displayed a columnar dendritic structure with enhanced mechanical properties [18]. Furthermore, the adoption of AM technology and practices has been explored, focusing on their impact on mechanical properties, microstructures, and welding parameters [19].

Optimization studies on WAAM techniques, such as activated tungsten inert gas welding, have been conducted to identify ideal welding process parameters for specific plate thicknesses [19]. Discussions on WAAM techniques and commonly used metallic feedstock materials emphasize the cost-effectiveness and efficiency of wire-based AM compared to powder-based AM for producing large structural metallic components [20] and [21]. Following the GTAW of the WAAM process, a solution annealing process at 980 °C for two hours is employed to dissolve secondary phases further enhancing the mechanical qualities. Subsequently, water quenching is utilized to rapidly cool the material, preventing the formation of new secondary phases and improving tensile qualities. In summary, the WAAM production method for Inconel 625 alloy, incorporating the GTAW process, solution annealing, and water quenching, consistently delivers high-quality, mechanically sound parts suitable for diverse industrial applications. The significance of selecting 980 °C and a 2-hour duration for annealing WAAM-printed Inconel 625 alloy lies in the observed effects on material properties. Research indicates that annealing at 980 °C for 2 hours increases the yield strength of the material. Specifically, the yield strength remains stable up to 1 hour of annealing but exhibits growth after the 2-hour heat treatment. Additionally, this annealing process is linked to the dissolution of a significant amount of the Laves phase and the precipitation of the δ phase, signifying a substantial impact on the material's microstructure. Moreover, the annealing conditions have been associated with the absence of softening behavior in Inconel 625 at 980 °C, in contrast to the observed softening at 1050 °C. Therefore, the deliberate choice of 980 °C and 2 hours for annealing is crucial due to its profound influence on the mechanical properties and microstructure of WAAM-printed Inconel 625, ultimately shaping the material's strength and behavior [16], [22], and [23].

In the realm of AM, particularly with WAAM utilizing the GTAW process, the current research aims to delve into the microstructural and mechanical characterization of Inconel 625. This nickel-based super alloy, renowned for its remarkable corrosion resistance and high strength, plays a pivotal role in diverse industries, including aerospace, chemical processing, and marine engineering. The novelty of this study lies in its comprehensive exploration of the effects of heat treatment on Inconel 625 additively manufactured through WAAM with the GTAW process. By investigating crucial parameters, the research not only contributes to the understanding of the manufacturing process but also delves into the intricate details of post-processing techniques. The incorporation of solution annealing at 980 °C offers a unique perspective on enhancing mechanical qualities and mitigating the formation of secondary phases. This novel approach promises to provide valuable insights into optimizing the production of high-quality, mechanically robust Inconel 625 components, advancing the field of AM with practical implications for various industrial applications.

## 2 METHODS AND MATERIALS

A Gantry semiautomatic welding robot and a Fronius TPS 400i LSC ADV power source are utilized to complete the WAAM process, which was employed to construct the multilayer wall structure using the GTAW method, as shown in Fig. 1. The multilayer wall structures are additively welded onto a base plate made of Inconel 625 alloy with a thickness of 13 mm. To determine the elemental composition of the base plate, an optical emission spectroscopy (OES) test is performed. Table 1 displays the elemental compositions found in the base plate.


(a) (b)

**Fig. 1.** Images of a) GTAW welding machine setup with gantry, and b) WELDING TORCH nozzle and WAAM printed multi-layered wall

**Table 1.** Chemical composition of Inconel 625 Alloy

| Elements | Si | Mn | Cr | Mo | Nb | Fe | Ni |
|---|---|---|---|---|---|---|---|
| wt. % | 0.27 | 0.25 | 21.12 | 8.84 | 3.80 | 4.26 | 60.15 |

The substrate was machined using a grinding machine and cleaned with acetone to get rid of faults and ensure a flawless weld structure. The process parameters considered were: current of 220 V, travel speed of 90 mm/min, and filler wire feed speed of 380 mm/min. The voltage was kept between 12 V and 14 V. The plate is firmly fixed on the fixture after the parameters are established to avoid distortion. Using a 3.2 mm diameter thoriated tungsten electrode that cannot be consumed, the base metal is fused to create the molten pool. To construct the thin-walled component, a molten pool was formed in the base plate and filled with Inconel 625 alloy filler wire with a 1.2 mm diameter using a GTAW method based on WAAM technology. The shielding gas used throughout the deposition procedure was pure 99.99 % argon inert gas with a flowing at a rate of 15 l/min.

By using the selected process parameter, the thin multilayer wall structure is built layer by layer. By keeping a cooling period of 120 seconds between succeeding layer depositions, the interlayer temperature was decreased to room temperature. As shown in Fig. 1b, the multilayer wall structure was built, which has 10 mm thickness, 66 mm height, and 120 mm length.

### 2.1 Heat Treatment Process

A muffle furnace, a kind of furnace that delivers homogeneous heating of the material, is commonly used for the heat treatment process. This makes it easier to make sure that the whole material is heated to the needed temperature and maintained there for the necessary amount of time, leading to a more uniform microstructure throughout the material. The material is heated to a certain temperature, with 980 °C, and maintained at that temperature for a specific amount of time 2 hours, throughout the heat treatment process [23] and [24]. Based on the material being annealed and the required qualities, this temperature and time are carefully selected [12]. Overall, the solution annealing procedure is a crucial step in producing high-quality Inconel 625 weldments made by WAAM since it helps to enhance the material's mechanical qualities and make sure it satisfies the specifications of several industrial applications.

### 2.2 Specimen Processing and Characterization

The top and bottom zones of the fabricated multilayer wall structure's microstructure, mechanical properties, and fractography morphologies were then examined in two states: as-deposited and heat-treated condition.

Samples from the top and bottom zones of the multilayered wall structure are obtained, each measuring 10 mm by 10 mm, to perform a microstructural examination. The extracted samples are polished to a mirror-like finish without any noticeable scratch marks using coarse and fine grid emery sheets. Sample specimens are electrolytically etched for 15 to 20 seconds while connected to the direct current (DC) supply using 2.1 grams of oxalic acid mixed with 200 milliliters of distilled water. To obtain the samples' microstructures, etched samples were analyzed for microstructure under an optical microscope and with a SEM at various magnifications and locations in as-deposited and heat-treated condition.

The top and bottom zones of the constructed multilayer wall structure were subjected to tensile, fractography, and microhardness tests, both in as-deposited and heat-treated condition. The American Society for Testing Materials (ASTM) E8 standard's tensile test was carried out using a Universal Testing Machine (UTM) 600 kN [25]. The tensile specimens are extracted from the multi-layered wall structure using wire-cut EDM machining process. This test is used to determine the metallic material's tensile strength, yield strength, and ductility.

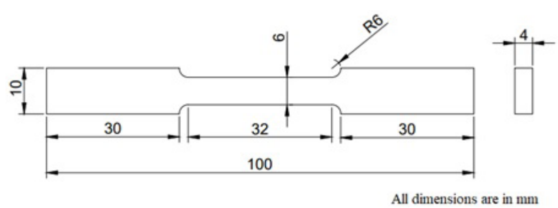


Fig. 2. Schematic of Tensile specimen dimensions as per ASTM - E8 standard [25]

The dimensions of the tensile specimen according to the ASTM E8 standard are displayed in Fig. 2 Also, the fractography test on the fractured surface of the broken tensile specimen was analyzed in the SEM system to better understand the properties of the fractured surface. To determine the hardness of the samples from the created multilayer wall structure in as-deposited and heat-treated condition, a microhardness test was carried out in the Vickers hardness machine with a force of 1 kg.

## 3 RESULT AND DISCUSSIONS

### 3.1 Physical Characteristics

The GTAW process's semi-automatic welding robot deposits the multilayer wall structure, which consists of 42 layers with a height of 65 mm and a length of 120 mm. Due to the unidirectional deposition technique, building and collapse are seen at the beginning and end of deposition in the produced multilayer wall structure, as shown in Fig. 3.

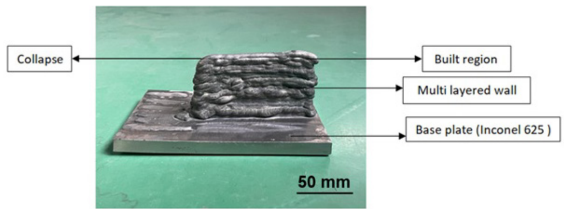


Fig. 3. Image of WAAM printed Inconel 625 Multilayer wall structure

The built zone reaches its maximum height in comparison to the collapse region as the number of layers rises. This leads to inaccurate deposited component dimensions. This issue is fixed by adding extra passes at the wall's end point to maintain an equal height between the starting and ending points.

### 3.2 Microstructural Analysis

An optical microscope (OM) and a SEM were used to conduct a microstructural study on the sample in order to understand the underlying changes in phases and grain structure morphology in the top and bottom zones of the constructed multilayer wall structure in as-deposited and heat-treated conditions. The constructed multilayer wall structure exhibits the effective grain structure.

#### *3.2.1 Optical Microstructure as-Deposited Condition*

The top and bottom zones of the created multilayer wall structure's optical microstructure pictures in their as-deposited form are depicted in Fig. 4.

Most of the heat input during the WAAM process is lost by convection and radiation to the surrounding atmosphere. The bottom layer has efficient heat conduction because of the heat being transported away through the substrate as well; as a result, solidification happens quickly. Equiaxed blocky-like structure and crystallite morphology are only practically feasible at very low temperature gradient levels. The rate of solidification, however, is slower at the top of the formed structure than it is at the bottom because of the slow heat transfer. The observed microstructure has varied in various areas of the deposit because of this difference in thermal behavior during the additive welding process. The microstructure in the top zone appears to be layered, and the deposited layer can be identified by elongated crystallites, as shown in Fig. 4a. The equiaxed blocky structure in the bottom zone of the multilayer wall structure is shown in Fig. 4b due to the varied solidification rates. Moreover, gamma phases are only present in the top zone of the multilayer wall structure, while secondary phases can be found in both the top and bottom zones of the built structure. These secondary phases' generation and distribution in Inconel 625 produced by WAAM can be influenced by several process variables, including heat input and cooling rate. Controlling these variables is crucial for reducing the production of detrimental phases and improving the material's properties for the intended application. This can be achieved by performing a heat treatment process.

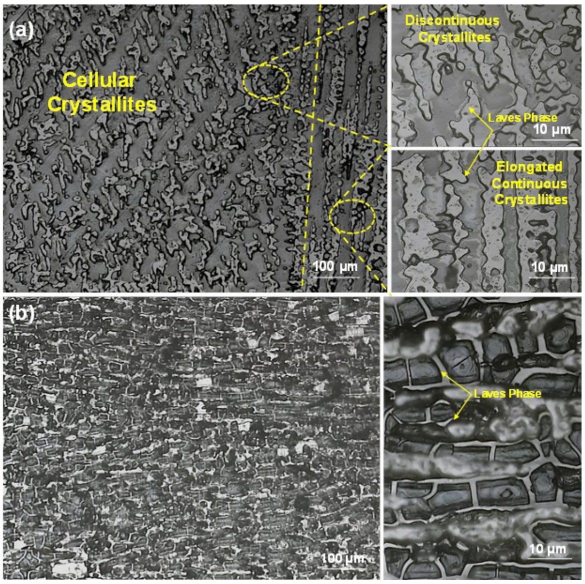


**Fig. 4.** Optical microstructure of Inconel 625 alloy in as – WAAM deposited condition from: a) top zone, and b) bottom zone

### 3.2.2 *Optical Microstructure with Heat Treatment*

After heat treatment, it is found that there is an elimination of secondary phases that can lead to a more homogeneous microstructure in both the top and bottom zones of the multilayer wall structure**.** Improvements in mechanical characteristics and microstructure can all be attained through the disappearance of secondary phases after heat treatment of multilayer wall structures.

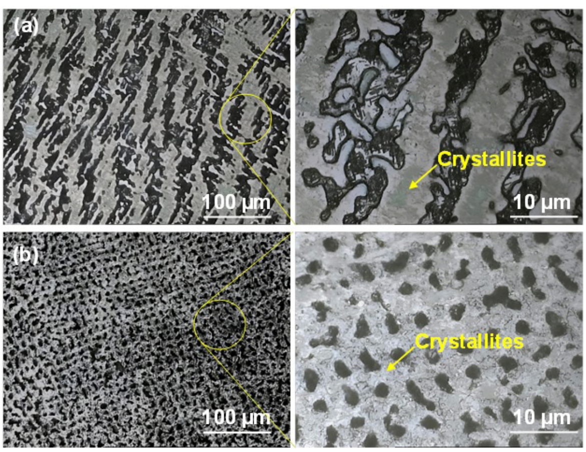


**Fig. 5.** Optical microstructure of Inconel 625 alloy in WAAM deposited and post heat treated condition from: a) top zone, and b) bottom zone

Due to recrystallization occurring during the heat treatment process in the bottom zone of the built structure, the microstructure changes from the blocky structure to the refined grain structure, as shown in Fig. 5b. Moreover, there is less uniaxial segregation of microstructure. After heat treatment, the precipitates in the microstructure were dissolved, and evenly distributed re-precipitation occurred.

Overall, recrystallization is encouraged by the heat treatment process, which also improves the microstructure, and produces finer, more equiaxed grains and better material properties. As a result, components made in as-deposited and heat treated condition using Inconel 625 WAAM have different optical microstructures. The blocky microstructure of Inconel 625 also changes into a fine-grained one after heat treatment, which enhances the material's mechanical properties.

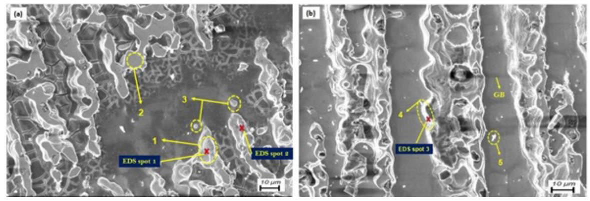


**Fig. 6.** SEM image of: a) top zone as-deposited condition alloy by WAAM manufacturing, and b) bottom zone as-deposited condition alloy by WAAM manufacturing

To understand the microstructure in its as-deposited condition, a SEM image at higher magnification, as shown in Fig. 6 was utilized. The top zone of the constructed multilayer wall structure's zones 1 and 2 (Fig. 7a and b) revealed by EDS analysis has a composition that is nearly identical to that of the Inconel 625 alloy's primary phase, the Ni-based matrix. This composition amply demonstrates the solute segregation with the erratic bright patches known as the 'laves phase' and the small particle sizes also visible in the microstructure image, which is identified as MC carbides. The EDS data presented in Fig. 7d further elucidates the elemental distribution across three spots, showing the following weight percentages.

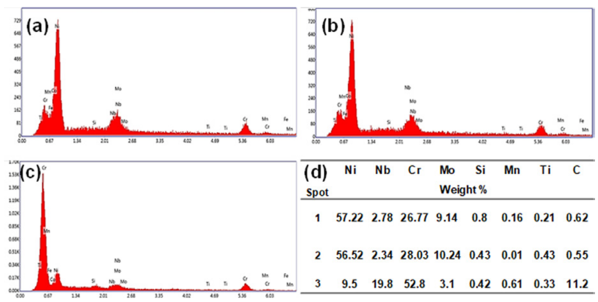

| (d) Spot | Ni | Nb | Cr | Mo | Si | Mn | Ti | C |
|---|---|---|---|---|---|---|---|---|
| | Weight % | | | | | | | |
| 1 | 57.22 | 2.78 | 26.77 | 9.14 | 0.8 | 0.16 | 0.21 | 0.62 |
| 2 | 56.52 | 2.34 | 28.03 | 10.24 | 0.43 | 0.01 | 0.43 | 0.55 |
| 3 | 9.5 | 19.8 | 52.8 | 3.1 | 0.42 | 0.61 | 0.33 | 11.2 |

**Fig. 7.** EDS spectra from: a) spot 1 of top zone, b) spot 2 of top zone, c) spot 3 of bottom zone, and d) elemental analysis at the spots

The Cr-rich M23C6 carbides at the grain boundaries were confirmed by the EDS image in Fig. 7c, according to a spot examination of the bottom zone. Further the EDS data indicates a high niobium content in Spot 3 suggests the formation of MC carbides, which are critical for enhancing the strength and stability of the alloy at elevated temperatures.

Fig. 8 displays the presence of delta precipitates, which are formed due to the dissolution of secondary phases like laves phase, gamma matrix, and MC carbides.

The dissolution of secondary phases is clear by the EDS spot analysis, which is shown in Fig. 9 on the top and bottom zones of the multilayer wall structure, and some of the secondary phases are undissolved, which results in the reduction of ductility after the heat treatment process of additively deposited Inconel 625 alloy. Notably, the chromium (Cr) content is significantly higher in the bottom zone (34.04 %) compared to the top zone (20.79 %), which may enhance corrosion resistance and strength. Additionally, niobium (Nb) is much lower in the bottom zone (2.34 %) than in the top zone (11.32 %), potentially explaining the observed decrease in ductility.

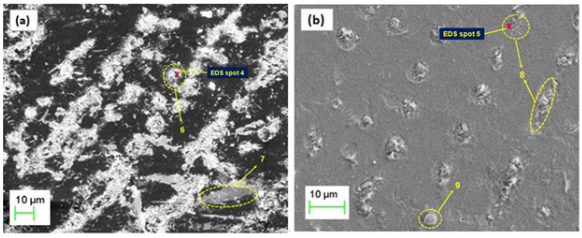


Fig. 8. SEM microstructure of WAAM printed Inconel 625 alloy from: a) top zone heat treated condition, and b) bottom zone heat treated condition

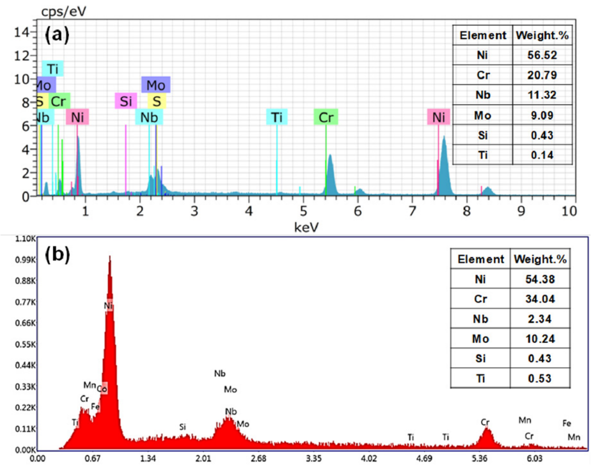


Fig. 9. EDS spectra from: a) spot 4 of the top zone after heat treated condition, and b) spot 5 of the top zone after heat treated condition

## 3.3 Mechanical Characteristics

To analyze the mechanical property of the multilayer wall structure, a tensile test was taken on the top and bottom zones. Additionally, a fractography test was carried out in the fractured zone of the tensile specimen to correlate the results of the mechanical and microstructural property tests. Microhardness tests were also carried out. These tests were carried out both in as-deposited and heat-treated condition in the top and bottom zones of the built multilayer wall structure.

### 3.3.1 Tensile Test

The top and bottom zones of the multilayer wall structure's tensile specimens, as per ASTM-E8 standard dimensions, were extracted using wire cut EDM and tested using a universal testing machine (UTM) under two different conditions: as-deposited and heat-treated. Tensile test data, including yield strength, elongation, and tensile strength, are displayed in Table 2. In the as-deposited condition, the yield strength of the Inconel 625 alloy ranges from 340 MPa to 394 MPa, with the top zone exhibiting slightly higher values than the bottom zone. This variation is likely due to differences in cooling rates and thermal gradients during the deposition process. The tensile strength also shows notable differences between the top and bottom zones, with values ranging from 527 MPa to 623 MPa. The elongation percentage was observed to be higher in the bottom zone (59 %) compared to the top zone (53 %), suggesting a more ductile microstructure in the bottom region, possibly due to lower residual stresses or a more favorable grain structure.

According to the results of the tensile tests, the yield strength and tensile strength in the top and bottom zones are improved by 15 % and 22 % and 17 % and 38 %, respectively, after the heat treatment process. Specifically, the yield strength increases to 457 MPa in the top zone and 416 MPa in the bottom zone, which aligns with literature data, suggesting that heat treatment promotes precipitation strengthening and the relaxation of residual stresses, leading to improved yield strength. The tensile strength also improves significantly, reaching approximately 729 MPa in both zones. However, the elongation percentage decreases after heat treatment, with the top zone showing 43.5 % and the bottom zone 47 %. This reduction in elongation could be attributed to the formation of precipitates that hinder dislocation movement, resulting in increased strength but reduced ductility. The comparison with literature data indicates that the mechanical properties of Inconel 625 fabricated using WAAM are competitive with traditional methods such as casting.

### 3.3.2 Fractography Test

The fractured surface of the tensile specimen was analyzed by using SEM is shown in the Fig. 10a and b which represents the top and bottom zones of multilayer wall structure in as-deposited condition, whereas Fig. 10c and d represents the top and bottom zones with heat treated condition. Fractography test was conducted using the fractured tensile specimen to identify the connection between the microstructure and the mechanical properties.

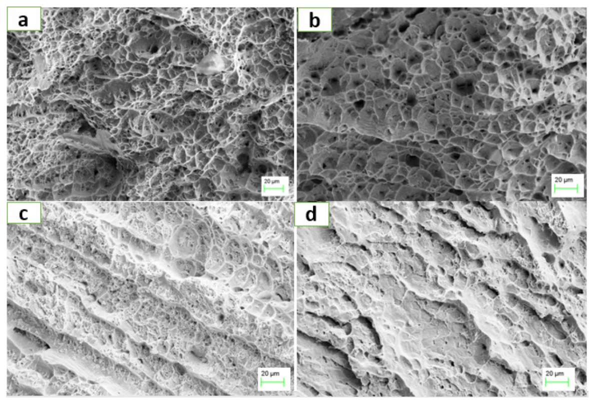


Fig. 10. Fractography micrograph of: a) and b) samples in as-deposited condition, and c) and d) in heat treated condition of top and bottom zone of the multilayer wall structure

The deep dimples in the as printed samples corroborates the occurrence of micro void coalescence and associated ductile fracture with an elongation of 50 % to 60 %. However, on the other hand, the

Table 2. Tensile test results of as deposited and post printing heat treated Inconel 625 alloy

| Mechanical properties | As deposited | | | Heat treated | | | As cast |
|---|---|---|---|---|---|---|---|
| | Top zone | Bottom zone | Literature data [9], [10], [26] | Top zone | Bottom zone | Literature data [9], [10], [26] | |
| Yield strength [MPa] | 394 ± 12 | 340 ± 08 | 376.9 to 400.8 | 457 ± 11 | 416 ± 6 | 414 to 615 | 350 |
| Tensile strength [MPa] | 623 ± 11 | 527 ± 09 | 647.9 to 687.7 | 729 ± 8 | 728 ± 11 | 827 to 1024 | 710 |
| Elongation [%] | 53 ± 5 | 59 ± 2 | 43 to 46.5 | 43.5 ± 4 | 47 ± 4 | 30 to 60 | 40 |

heat treated sample shows a shallow dimples with plateau formation, which indicates the chances of localized plastic deformation and inter-granular cracking along with a minimal amount of micro-void coalescence. Similar observations were reported in welding studies of Ramor 500 Armor Steel [27] and [28]. Further studies are required to understand the mechanism.

### 3.3.3 Microhardness Test

The built multilayer wall structure's top and bottom zones were measured for microhardness using the Vicker's hardness testing machine under two conditions: as-deposited and heat treated. Table 3 displays the results that were obtained. The hardness values for the samples that were heat-treated and that were as-deposited is appear to have undergone minimal change. However as compared to the top and bottom zone of the constructed multilayer wall structure, the hardness value in the bottom zone has improved in both the conditions. When compared to the literature data, the hardness values from the present study is higher than the reported ranges of 145 HV to 220 HV for the annealed condition and 243 HV to 247 HV for the as printed condition. This indicates that the multilayer wall structure in the current investigation demonstrates enhanced hardness properties relative to previously documented results.

**Table 3. Microhardness of WAAM deposited Inconel 625 alloy in as-deposited and heat-treated condition**

| Mechanical properties Micro-hardness (HV) | Heat treated condition | | As-deposited condition | |
|---|---|---|---|---|
| | Top zone | Bottom zone | Top zone | Bottom zone |
| Present study | 215.9 ± 09 | 273.8 ± 08 | 209.4 ± 04 | 287 ± 06 |
| Literature data [10] | 145 to 220 | | 243 to 247 | |

## 4 CONCLUSIONS

The Inconel 625 alloy multi-layered wall construction underwent unidirectional GTAW welding, resulting in decreased height at the end of the process, necessitating additional passes for dimensional accuracy. Following a 2-hour heat treatment at 980 °C, the microstructure exhibited fine dentrites, a transformation from discontinuous and elongated dentrites. The multilayer wall structure primarily comprised Ni-Cr matrix-based gamma phase, laves phases, and MC carbides, dissolved through the heat treatment process. This treatment led to a 17 % to 38 % improvement in ultimate tensile strength and yield strength in the top zone and a 15 % to 22 % enhancement in the bottom zone, attributed to delta precipitate formation and laves phase dissolution. While the average microhardness showed no significant change post-heat treatment, the bottom zone exhibited a higher microhardness value compared to the top zone.

## REFERENCES


[1] Nguyen, H.D., Pramanik, A., Basak, A.K., Dong, Y., Prakash, C., Debnath, S., Buddhi, D. A critical review on additive manufacturing of Ti-6Al-4V alloy: Microstructure and mechanical properties. J Mater Res Technol 18 4641-4661 (2022) **DOI:10.1016/j.jmrt.2022.04.055**

[2] Korkmaz, M.E., Waqar, S., Garcia-Collado, A., Gupta, M.K., Krolczyk, G.M. A technical overview of metallic parts in hybrid additive manufacturing industry. *J Mater Res Technol* 18 384-395 (2022) **DOI:10.1016/j.jmrt.2022.02.085**

[3] Günen, A., Gürol, U., Koçak, M., Cam, G. A new approach to improve some properties of wire arc additively manufactured stainless steel components: Simultaneous homogenization and boriding. *Surf Coat Technol* 460 129395 (2023) **DOI:10.1016/j.surfcoat.2023.129395**

[4] Gürol, U., Altınay, Y., Günen, A., Bölükbaşı, Ö.S., Koçak, M., Çam, G. Effect of powder-pack aluminizing on microstructure and oxidation resistance of wire arc additively manufactured stainless steels. *Surf Coat Technol* 468 129742 (2023) **DOI:10.1016/j.surfcoat.2023.129742**

[5] Pan, Z., Ding, D., Wu, B., Cuiuri, D., Li, H., Norrish, J. Arc welding processes for additive manufacturing: a review. *Trans Intell Weld Manuf* 1 3-24 (2018) **DOI:10.1007/978-981-10-5355-9_1**

[6] Chintala, A., Tejaswi Kumar, M., Sathishkumar, M., Arivazhagan, N., Manikandan, M. Technology development for producing Inconel 625 in aerospace application using wire arc additive manufacturing process. *J Mater Eng Perform* 30 5333-5341 (2021) **DOI:10.1007/s11665-021-05781-6**

[7] Owais M., Mridul J., Noor W., N.H. Wire arc additive manufacturing (WAAM) of Inconel 625 Alloy and its microstructure and mechanical properties. *Int Res J Eng Technol* 08 1518-1528 (2021)

[8] Geng, H., Li, J., Xiong, J., Lin, X., Zhang, F. Optimization of wire feed for GTAW based additive manufacturing. *J Mater Process Technol* 243 40-47 (2017) **DOI:10.1016/j.jmatprotec.2016.11.027**

[9] Ferreira, A.A., Reis, A.R., Amaral, R.L., Cruz, J.M., Romio, P.C., Seabra, J.O., et al. Mechanical and microstructural characterisation of bulk Inconel 625 produced by direct laser deposition. *Mater Sci Eng A* 838 142777 (2022) **DOI:10.1016/j.msea.2022.142777**

[10] Yuan, X., Qiu, H., Zeng, F., Luo, W., Li, H., Wang, X. et al. Microstructural evolution and mechanical properties of Inconel 625 superalloy fabricated by pulsed microplasma rapid additive manufacturing. *J Manuf Process* 77 63-74 (2022) **DOI:10.1016/j.jmapro.2022.03.008**

[11] Wang, X., Wang, A., Wang, K., Li, Y. Process stability for GTAW-based additive manufacturing. *Rapid Prototyp J* 25 809-819 (2019) **DOI:10.1108/RPJ-02-2018-0046**

[12] Thakur, P.P., Chapgaon, A.N. A review on effects of GTAW process parameters on weld. *IJRASET* 4 136-140 (2016) **DOI:10.13140/RG.2.2.11535.38569**

[13] Kumar, S.P., Elangovan, S., Mohanraj, R., Ramakrishna, J.R. A review on properties of Inconel 625 and Inconel 718 fabricated using direct energy deposition. *Mater Today: Proc* 46 7892-7906 (2021) **DOI:10.1016/j.matpr.2021.02.566**

[14] Hack, H., Link, R., Knudsen, E., Baker, B., Olig, S. Mechanical properties of additive manufactured nickel alloy 625. *Addit Manuf* 14 105-115 (2017) **DOI:10.1016/j.addma.2017.02.004**

[15] Yangfan, W., Xizhang, C., Chuanchu, S. Microstructure and mechanical properties of Inconel 625 fabricated by wire-arc additive manufacturing *Surf Coat Technol* 374 116-123 (2019) **DOI:10.1016/j.surfcoat.2019.05.079**

[16] Tanvir, A.N.M., Ahsan, M.R., Ji, C., Hawkins, W., Bates, B., Kim, D.B. Heat treatment effects on Inconel 625 components fabricated by wire+ arc additive manufacturing (WAAM)-part 1: microstructural characterization. *Int J Adv Manuf Technol* 103 3785-3798 (2019) **DOI:10.1007/s00170-019-03828-6**

[17] Akselsen, O.M., Bjørge, R., Ånes, H.W., Ren, X., Nyhus, B. Microstructure and properties of wire arc additive manufacturing of Inconel 625 *Metals* 12 1867 (2022) **DOI:10.3390/met12111867**

[18] Mohan Kumar, S., Rajesh Kannan, A., Pravin Kumar, N., Pramod, R., Siva Shanmugam, N., Vishnu, A.S., Channabasavanna, S.G. Microstructural features and mechanical integrity of wire arc additive manufactured SS321/Inconel 625 functionally gradient material. *J Mater Eng Perform* 30 5692-5703 (2021) **DOI:10.1007/s11665-021-05617-3**

[19] Kumar, S.S., Maheswaran, C.B., Kannan, T.D.B. Experimental investigation on a pulsed TIG welding of Inconel 625. *Mater Today: Proc* 45, 2109-2114 (2021) **DOI:10.1016/j.matpr.2020.09.724**

[20] Guo, C., Ying, M., Dang, H., Hu, R., Chen, F. Microstructural and intergranular corrosion properties of Inconel 625 superalloys fabricated using wire arc additive manufacturing. *Mater Res Express* 8 035103 (2021) **DOI:10.1088/2053-1591/abe977**

[21] Ravi, G., Murugan, N., Arulmani, R. Microstructure and mechanical properties of Inconel-625 slab component fabricated by wire arc additive manufacturing. *Mater Sci Technol* 36 1785-1795 (2020) **DOI:10.1080/02670836.2020.1836737**

[22] Karayel, E., Bozkurt, Y. (2020). Additive manufacturing method and different welding applications. *J Mater Res Technol* 911424-11438 **DOI:10.1016/j.jmrt.2020.08.039**

[23] Sivakumar, J., Vasudevan, M., Korra, N.N. (2020). Systematic welding process parameter optimization in activated tungsten inert gas (A-TIG) welding of Inconel 625. Trans Indian Inst Met 73 555-569 **DOI:10.1007/s12666-020-01876-1**.

[24] Dhinakaran, V., Ajith, J., Fahmidha, A.F.Y., Jagadeesha, T., Sathish, T., Stalin, B. (2020). Wire arc additive manufacturing (WAAM) process of nickel-based superalloys-A review. *Mater Today: Proc* 920-925 **DOI:10.1016/j.matpr.2019.08.159**

[25] Holt, J.M. *Uniaxial tension testing. In Mechanical Testing and Evaluation*. ASM International (2000) Materials Park
[26] Seow, C.E., Coules, H.E., Wu, G., Khan, R.H., Xu, X., Williams, S. Wire+ arc additively manufactured Inconel 718: Effect of post-deposition heat treatments on microstructure and tensile properties. *Mater Des* 183 108157 (2019) **DOI:10.1016/j.matdes.2019.108157**
[27] Günen, A., Gürol, U., Koçak, M., Çam, G. Investigation into the influence of boronizing on the wear behavior of additively manufactured Inconel 625 alloy at elevated temperature. *Prog Addit Manuf* 8 1281-1301 (2023) **DOI:10.1007/s40964-023-00398-8**
[28] Günen, A., Bayar, S., Karakaş, M.S. Effect of different arc welding processes on the metallurgical and mechanical properties of Ramor 500 armor steel. *J Eng Mater Technol* 142 021007 (2020) **DOI:10.1115/1.4045569**

**Received 2024-03-14, revised 2024-08-20, accepted 2024-10-03**
*Original Scientific Paper.*

**Data availability** *The data that support the findings of this study are available from the corresponding author upon reasonable request.*

**Author contributions** *Saravanakumar K contributed to conceptualization, formal analysis, investigation, methodology, and writing – original draft; Saravanan S provided supervision, project administration, writing – review & editing, and resources; Balaji VG contributed to data curation, validation and visualization.*

## Karakterizacija mikrostrukture in mehanskih lastnosti Inconela 625 po obločnem navarjanju z žico: učinki toplotne obdelave

**Povzetek** *Obločno navarjanje z žico (WAAM) je obetavna tehnika za izdelavo kompleksnih geometrij superzlitin na osnovi niklja, kot je Inconel 625. V pričujoči raziskavi smo analizirali mikrostrukturo in mehanske lastnosti zlitine Inconel 625, izdelane s postopkom obločnega varjenja s plinskim volframom (GTAW) v tehnologiji WAAM, da bi raziskali učinke toplotne obdelave na zgornjo in spodnjo cono večplastne stenske strukture. Vzorci so bili dve uri toplotno obdelani pri 980 °C, nato pa ohlajeni z vodo (žarjenje z raztopino). Po toplotni obdelavi mikrostruktura razkriva, da so najbolj pogoste faze, kot so laves, sekundarne faze (γ') in monokarbidi (MC), raztopljene, kar je jasno opazno z optično mikroskopijo (OM), skenirno elektronsko mikroskopijo (SEM) in energijsko disperzijsko spektroskopijo (EDS). Tudi po postopku toplotne obdelave mehanske lastnosti, kot so rezultati mikrotrdote, kažejo, da ima spodnja cona večplastne stenske strukture višjo vrednost trdote kot zgornja cona. Po odstranitvi sekundarnih faz s postopkom raztopinskega žarjenja sta se natezna trdnost in meja plastičnosti v zgornjem in spodnjem delu večplastne stenske strukture povečali za skoraj 17 % do 38 % oziroma 15 % do 22 %.*

**Ključne besede** *obločno navarjanje z žico (WAAM), toplotna obdelava, optični mikroskop, natezna trdnost*